Feasibility study of Raman spectroscopy for investigating the mouse retina in vivo

Suman K. Manna, Marcos A. S. de Oliveira, Pengfei Zhang, Ratheesh K. Meleppat, Che-Wei Chang, et al.

Suman K. Manna, Marcos A. S. de Oliveira, Pengfei Zhang, Ratheesh K. Meleppat, Che-Wei Chang, Edward N. Pugh, James W. Chan, Robert J. Zawadzki, "Feasibility study of Raman spectroscopy for investigating the mouse retina in vivo," Proc. SPIE 10474, Ophthalmic Technologies XXVIII, 104741J (19 March 2018); doi: 10.1117/12.2288790

SPIE.

Event: SPIE BiOS, 2018, San Francisco, California, United States

Feasibility Study of Raman Spectroscopy for Investigating the Mouse Retina *in vivo*

Suman K. Manna[1], Marcos A. S. de Oliveira[2], Pengfei Zhang[1], Ratheesh K. Maleppat[1], Che-Wei Chang[2], Edward N. Pugh Jr.[1], James Chan[2] and Robert J. Zawadzki[1,3]*

[1]UC Davis Eye-pod, Department of Cell Biology and Human Anatomy, University of California Davis, Davis, CA 95616

[2]Department of Pathology and Laboratory Medicine, University of California, Davis, 4400 V Street, Sacramento, California 95817

[3]UC Davis Eye Center, Dept. of Ophthalmology & Vision Science, University of California Davis, 4860 Y Street, Suite 2400, Sacramento, California 95817

*rjzawadzki@ucdavis.edu

ABSTRACT

The use of Raman spectroscopy in biochemistry has been very successful, particularly because of its ability to identify elementary chemical species. However, application of this spectroscopic technique for *in vivo* assessment is often limited by autofluorescence, which make detection of Raman signatures difficult. The mouse eye has been used as an optical testbed for investigation of a variety of disease models and therapeutic pathways. Implementation of *in vivo* Raman spectroscopy in mice retina would be valuable but needs to be examined in context of the intrinsic auto-fluorescence artifact and potential light damage if high probing beam powers were used. To evaluate feasibility, a Raman system was built on a custom SLO/OCT platform allowing mouse positioning and morphological data acquisition along with the Raman signal from a desired retinal eccentricity. The performance of the Raman system was first assessed with a model eye consisting of polystyrene in the image plane (retina), using excitation wavelengths of 488 nm, 561 nm, and 785 nm to determine whether auto-fluorescence would be reduced at longer wavelengths. To improve the SNR, the combined system is featured with the optical compatibility for these three excitations such that their corresponding spectra from a typical region of interest can be acquired consecutively during single imaging run. Our results include emission spectra acquired over 10 s with excitation energy less than 160 $J \cdot s^{-1} \cdot m^{-2}$ for all wavelengths and corresponding retinal morphology for different mouse strains including WT, BALB/c and ABCA4$^{-/-}$.

Keywords: Raman Spectroscopy, Auto-Fluorescence, Scanning Laser Ophthalmoscopy, Optical Coherence Tomography, Retinal Imaging, Multimodal System

1. INTRODUCTION

The physician's ability to diagnose disease is enhanced by the timely availability of objective, quantitative diagnostic information. Successive advances in biomedical technology have been driven by the need to provide such information. Novel biomedical applications of optical spectroscopy, such as fluorescence, reflectance and Raman scattering, can provide information about the composition of tissue at the molecular level. Of these techniques, Raman spectroscopy can provide the most detailed information about the chemical composition of the tissue under study. Since the progression of disease is accompanied by chemical change on cellular scale, Raman spectroscopy can provide the physician with valuable information for diagnosing disease. Moreover, since light can be delivered and collected rapidly via optical fibers, which can be incorporated into catheters, endoscopes, cannulas and needles, as necessary, Raman spectroscopy can be performed in vivo in real time. Along with these successful invasive detection techniques still there is a strong need to detect the Raman signature in a non-invasive manner specially for monitoring a disease at very early stage. Mouse eye has become an in situ optical testbed for investigation of a variety of ocular disease models and therapeutic pathways [1,2].

Ophthalmic Technologies XXVIII, edited by Fabrice Manns, Per G. Söderberg, Arthur Ho, Proc. of SPIE
Vol. 10474, 104741J · © 2018 SPIE · CCC code: 1605-7422/18/$18 · doi: 10.1117/12.2288790

Investigating Raman in this system is not only interesting for clinical assessment but also challenging for bio-photonics, enabling development of reliable protocol for ultrasensitive detection of Raman signature.

The major challenges of detection *in vivo* non-invasive Raman from mouse eye are power limitation of the Raman probe beam and focusing capability of the mouse eye. Raman emission intensity is proportional to the fourth power of the probe frequency, i.e., $I_R \propto I_0.n_i.\sigma(\gamma_{ex}).\gamma_{ex}^4.f(T)$, where, I_0 refers to incident beam irradiance, n_i-number density of the ith-state, $\sigma(\gamma_{ex})$ is the Raman scattering cross section (cm^{-2}), γ_{ex} the probe frequency, and $f(T)$ is the temperature dependent factor [3]. The above relationship reveals that shorter wavelengths generally provide stronger Raman signals. At the same time most of the biological tissues emit strong autofluorescence when excited by UV and short VIS wavelength, hence fluorescent background (noise for Raman signals) is increased, which makes detection of Raman signatures difficult. Techniques, including shifted excitation Raman difference spectroscopy (SERDS) [4], polarization modulation [5], Fourier transform filtering [6], temporal gating of fluorescence [7] and others, are potentially useful in overcoming this problem, but their applicability *in vivo* is challenging and so far, limited. Here, we discussed the feasibility of spontaneous retinal Raman spectroscopy *in vivo*. Towards that goal, a Raman system was built on a custom SLO/OCT platform (Fig.1), allowing mouse positioning and simultaneous morphological data acquisition along with the Raman signal from a desired retinal locus.

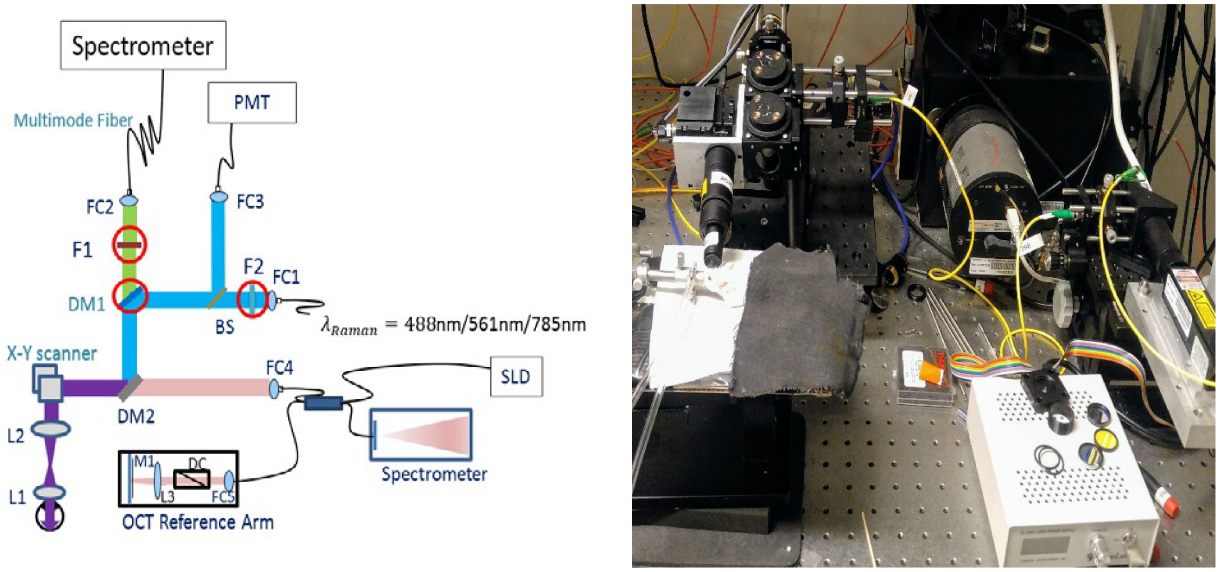

Figure 1. Experimental setup for in vivo Raman study, a. schematic diagram of the system showing Raman system in a combined imaging platform consists of SLO and OCT. The system is made compatible for three different Raman excitations at 488nm, 561nm and 785nm. b. image of the system under working condition.

The precise positioning and imaging capabilities of the combined SLO/OCT system make it possible to repeat Raman testing over several months, as needed for some therapeutic or diagnostic studies.

2. MATERIALS AND METHODS

2.1 Instruments

Raman spectra were collected by means of our custom designed instrument, optimized to collect Raman light emitted from a polystyrene by using three different excitation wavelengths 488nm, 561nm, and 785nm from OBIS laser from Coherent, Inc. The Raman illumination beam is passed through a notch filter to clean spectrum by rejecting side bands, if any are present. The collimated beam is directed on a dichroic beam splitter which has long pass transmission spectrum starting just after the excitation wavelength to collect all the Stokes Raman modes. After the dichroic, the beam is focused with a high NA (0.5) objective lens onto the sample. The excitation energy is restricted to 32 J·s^{-1}·m^{-2} for 488nm and 160 J·s^{-1}·m^{-2}

for 785 nm during the assessment of the system by using Polystyrene. Backscattered Raman light passed through a long pass filter followed by the dichroic filter and focused onto the collecting multimode fiber of core diameter 400μm and the NA of 0.39 which is matched with the collecting lens to have good beam coupling.

2.2 Mouse preparation:

Two different mouse strains -C57/Bl6J and Balb/c were used for this study. Mice were anesthetized using 1:4 oxygen and isoflurane gas mixture and thereafter placed on a positioning stage Fig.1b. The eye solutions- Tropicamide and Phenylephrine were used to dilate the eye and a lubricant eye gel was used for long time imaging without letting the eye dry. A temperature controller is used to maintain the temperature ~35℃ to avoid development of cold cataract.

2.3 Fluorescein staining:

Investigation of spontaneous Raman from two mouse strains are carried out with all the three excitation wavelengths. The result is presented in the next section. Briefly, the SNR of the spontaneous Raman is found to be low. Further, we have explored the possibility of enhancing spontaneous Raman signal by using extrinsic fluorescein as a contrast agent. Fluorescein is a biocompatible optically active dye. The typical absorption and emission bands are shown in Fig.2.

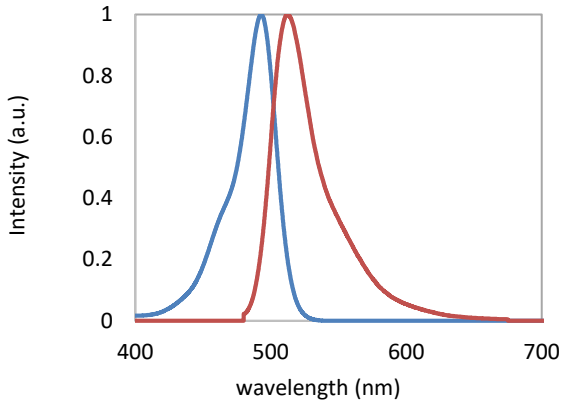

Figure 2 absorption and emission spectra of fluorescein.

The excitation wavelength of fluorescein is centered around 494nm. So, it is instructive to use Raman excitation wavelength well outside the fluorescein absorption band to avoid exciting phosphoresce. We used 785nm excitation for this purpose. The delivery of fluorescein in mouse eye is done by tail-vain injection and 15 minutes after the injection the mice are used for Raman spectroscopic study.

3. RESULTS

Our custom build Raman system on SLO-OCT platform is assessed with a known sample polystyrene with respect to all the Raman excitation wavelengths. The collimated beam is focused with a model eye with the replicated features of the mouse eye. The Raman emission form the polystyrene is plotted in Fig. 3. The acquisition time for all the experiments was kept the same, at 5s. Once we confirmed the system is recording all the characteristic Raman peaks, we move to image mouse eye in the same setup. A parallel acquisition of mouse fundus by SLO using Raman excitation wavelengths confirms the correct mouse positioning before start of Raman spectrum acquisition from smaller Region of Interest (ROI). Our imaging system also allows us to adjust depth focus to optimize the Raman signal from any layer of the retina.

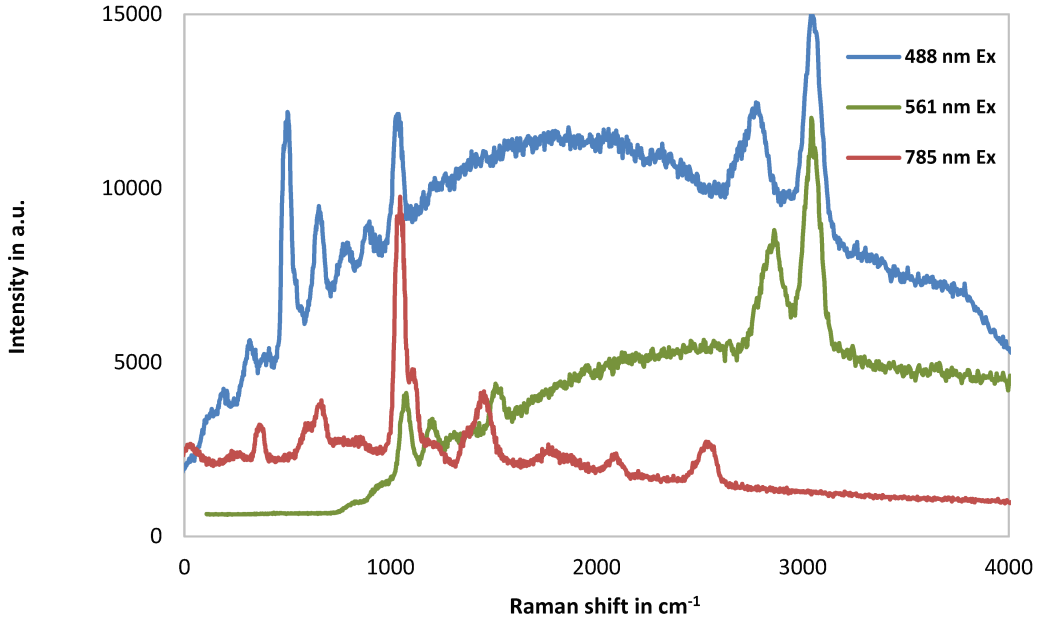

Figure 3. characteristic Raman signal from polystyrene, excited at three different wavelengths -488nm, 561nm and, 785nm. The acquisition time is same for all the cases which is 5s. A model eye consisting of the lens of NA 0.5 is used to focus the Raman excitation beam and the same spot is used to collect the Raman emission. All the excitations are used in situ without changing any optical component.

A typical SLO image and the Raman spectra are shown in Fig. 4. from two different mouse line C57/Bl6J, and Balb/c.

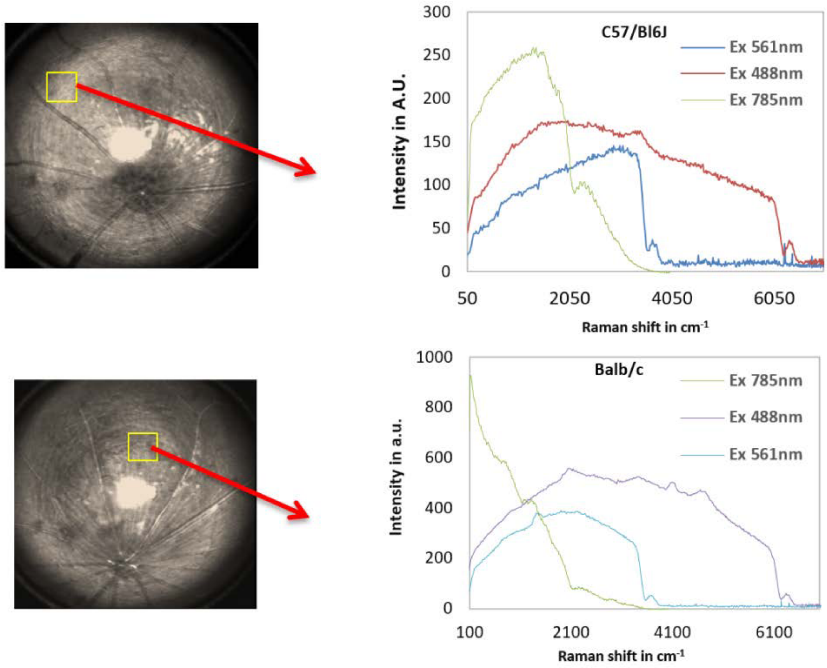

Figure 4. Raman spectra detected from retina of two different mice strains pigmented C57/Bl6J, and albino Balb/c; left panel shows SLO images of those eyes with the yellow rectangle depicting the ROI where spectra where acquired.

It is observed that the Raman spectra corresponding to 488nm and 561nm excitation are associated with strong fluorescence background compared to 785nm excitation. We have varied the location of the ROI in order to observe if

there is any strong Raman signal present. The fluorescent background spectral shape is found very similar over the entire retina. Further, we focus into different retina layers with a hope to obtain stronger signal. The Raman signals SNR in all the cases were very poor. The change in spectra observed in two mouse strains is mainly due to the fluorophores. In order to enhance the spontaneous Raman signal, we use a biocompatible contrast agent, fluorescein. Before we examine fluorescein in mouse eye, we measured the fluorescein Raman signal from a paper stained with fluorescein. The Raman spectrum of this fluorescein stained paper is plotted in Fig. 5a. The Raman spectrum of mouse retina 15 minutes after tail-vain fluorescein injection is found to be the same with the spectrum acquired before injection (Fig. 5b). It is also observed that even long acquisition time does not show any change except the overall background is increased. Note presence of fluorescein in the retina vasculature shown in the SLO fluorescence channel confirming successful injection of fluorescein.

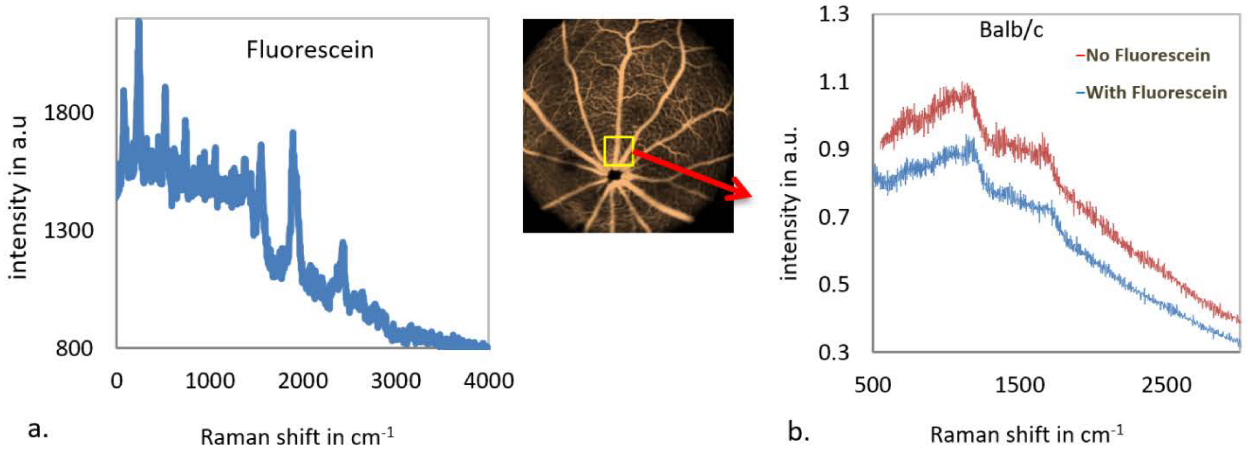

Figure 5. a). characteristic Raman signal from fluorescein excited with 785nm, b). characteristic Raman signal for excitation wavelength of 785nm from mouse retina before (red) and after fluorescein injection (blue). Middle image shows SLO mouse retina fluorescein angiography acquired during the same experiment.

4. CONCLUSIONS

In this manuscript several exploratory experiments testing feasibility of in vivo retinal Raman spectroscopy has been presented. Here is brief summary of our observations. Raman spectra plotted in Fig.3 show the excitation wavelength dependence of the fluorescence background. Although we observed an improvement in fluorescence background for longer excitation wavelengths, there is still relatively strong background even at 785nm excitation. The source of this background is most likely from the glass components of our system, which are reported to produce broadband Raman background [8]. Therefore, even for long excitation wavelength we didn't observed improvement of Raman signal SNR resulting in no clear in vivo Raman signature detected. To overcome this limitation, we tried to increase strength of Raman signal without increasing fluorescent background by using contrast agent (fluorescein). The graphs in Fig. 5 show that there is almost no contribution from the fluorescein broadband emission, because with and without fluorescein the background looks the same. There was however no Stoke Raman signature signal to be observed there as well.

In conclusion we believe that the lack of measurable Raman signal from the mouse eye in vivo might be due to the relatively low numerical aperture of probing and detecting Raman beams. We plan to test this in the future by implementing AO enhanced retinal imaging platform potentially improving Raman excitation and detection ratios. Additionally, we will try to improve our optics used for 785nm excitation to reduce broadband Raman background. Despite lack of success in detecting spontaneous Raman signals in mouse retinas, we think that potential benefit of working Raman probe will motivate further development and testing of new Raman imaging schemes that will be successful.

5. ACKNOWLEDGEMENT

Authors would like to acknowledge their funding sources: NSF I/UCRC CBSS Grant, NIH grants EY026556, and EY012576 (NEI Core Grant). This work was also partially supported by Barr Retina Research Foundation gift to UC Davis Department of Ophthalmology.

REFERENCES

[1] N. Okamoto, T. Tobe, S. F. Hackett, H. Ozaki, M. A. Vinores, W. LaRochelle, D. J. Zack, and P.A. Campochiaro, Transgenic mice with increased expression of vascular endothelial growth factor in the retina: a new model of intraretinal and subretinal neovascularization, Am. J. Pathol., 1997, 151, 281-291.

[2] C Portera-Cailliau, JC Hedreen, DL Price and VE Koliatsos, Evidence for apoptotic cell death in Huntington disease and excitotoxic animal models, J. Neuroscience, 1995, 15, 3775-3787.

[3] Stender AS, Marchuk K, Liu C, Sander S, Meyer MW, Smith EA, Neupane B, Wang G, Li J, Cheng J-X et al., Single cell optical imaging and spectroscopy, Chem. Rev. 2013, 113, 2469-2527.

[4] Cheng J-X, Xie XS, Vibrational spectroscopic imaging of living systems: an emerging platform for biology and medicine, Science 2015, 350.

[5] Shreve AP, Cherepy NJ, Mathies RA., Effective rejection of fluorescence interference in Raman spectroscopy using a shifted excitation difference technique, Appl. Spectrosc. 1992, 46, 707.

[6] Angel SM, DeArmond MK, Hanck KW, Wertz DW, Computer-controlled instrument for the recovery of a resonance Raman spectrum in the presence of strong luminescence, Anal. Chem. 1984, 56, 3000.

[7] Mosier-Boss PA, Lieberman SH, Newbery R., Fluorescence rejection in Raman spectroscopy by shifted-spectra, edge detection, and FFT filtering techniques, Appl. Spectrosc. 1995, 49, 630.

[8] Deffontaine A, Delhaye M, Bridoux M., In Time-resolved Vibrational Spectroscopy, Laubereau A, Stockburger M (eds). Springer: Berlin, 1985, 20–24.